Trajectory-Adaptive, Cost-Based Power Management Optimization for Regional Hybrid-Electric Aircraft Over Sequential Operations

Emma Cassidy, Yipeng Liu, Kathryn Kirsch, Max Z. Li, and Gokcin Cinar

***Abstract*—Hybrid-Electric Aircraft (HEA) present a potential pathway to enhance propulsive efficiency and reduce operating costs in regional airline operations. This study introduces a trajectory-adaptive power management strategy that optimizes allocation of electric and gas turbine engine power across sequential daily flights while addressing operational constraints such as limited gate charging durations and available ground time. HEA models are developed using physics-based and data-driven methods within the open-source Future Aircraft Sizing Tool (FAST). In contrast to prior studies that rely on fixed power splits or single-mission strategies, the proposed approach dynamically adjusts power distribution across mission phases to maximize efficiency and performance over a range of missions. Key findings indicate that sequence-optimized power management achieves an approximate 3% reduction in fuel burn and a 2% reduction in flight energy cost compared to a conventional baseline. The analysis uses a modeled HEA with conservative battery technology assumptions of 250 Wh/kg pack-level specific energy and a 150 kW charging power limit to reflect the capabilities of current technology. The study also finds that optimizing power allocation across a full day of operations yields greater benefits than optimizing each flight independently. Minimizing for either fuel burn or energy cost yields similar power management strategies, as fuel consumption is the dominant factor in the direct operating costs for the scenarios studied. These results demonstrate the feasibility of HEA integration into regional airline markets, offering improved operational efficiency and cost savings while maintaining compatibility with existing fleet schedules.**

***Index Terms*—electrified propulsion, optimal power management strategies, trajectory-adaptive control, cost-aware optimization**

I. Introduction

Hybrid-Electric Aircraft (HEA) present a promising alternative to conventional aircraft by offering improved fuel efficiency and reduced operating costs [2], [3]. However, effective HEA design must integrate operational constraints during the early stages of conceptual development to ensure compatibility with existing airline fleets. A significant challenge arises from the limitations of current lithium-ion battery technology, whose specific energy (0.20–0.25 kWh/kg) is nearly 50 times lower than that of jet fuel (11.9 kWh/kg). Although recent breakthroughs in research have demonstrated lithium-based batteries with specific energies exceeding 700 Wh/kg [4], such technology is neither commercially available nor sufficient to support fully electric aircraft. Electrified regional, narrow-body, and wide-body aircraft would require battery specific energies of approximately 600, 820, and 1,280 Wh/kg, respectively [5]. These limitations necessitate optimization-focused approaches that identify the most effective use cases and operational strategies for near-term HEA adoption.

The regional jet market is particularly promising for HEA integration due to its shorter-range missions, which better align with moderate battery utilization [6]–[8]. Nonetheless, replacing conventional aircraft with HEA on regional routes may increase airline operating costs unless substantial fuel savings can be achieved [9], [10]. In 2019, fuel accounted for nearly 24% of global airline operating costs [11], underscoring the importance of pursuing any strategies that can reduce fuel consumption and thus improve economic viability.

In parallel-hybrid architectures, strategies that reduce gas turbine takeoff power by incorporating short boosts of electric motor support have been shown to decrease fuel consumption [12]. Yet, without adaptive power management, extending hybridization beyond the takeoff phase often increases energy requirements and necessitates heavier batteries [2]. This additional battery mass increases gross takeoff weight and, in turn, the overall mission energy demand. Moreover, gate charging durations—constrained by conventional turnaround times—can further limit the realized benefits of hybridization [13]. An adaptive strategy that maximizes available battery energy is therefore essential to balance efficiency, cost, and feasibility.

Prior research on HEA power management has primarily focused on propulsion architecture types and high-level charge-depleting/sustaining strategies [14]–[16]. While optimization of power-split strategies has been explored [17], most studies hold the flight path and mission profile fixed to those of a conventional aircraft. When optimization is applied, the mission is typically discretized into only a few broad segments (e.g., climb, cruise, descent), limiting the granularity of possible power management strategies [18]–[20]. By contrast, this work

E. Cassidy and Y. Liu are with the Department of Aerospace Engineering, University of Michigan, Ann Arbor, MI, USA (e-mail: emmasmit@umich.edu; yipenglx@umich.edu). Corresponding author: Emma Cassidy. 1320 Beal Ave Ann Arbor, MI (925)286-9122).

K. Kirsch is with Thermofluid Sciences, RTX Technology Research Center, East Hartford, CT, USA (e-mail: kathryn.kirsch@rtx.com).

M. Z. Li and G. Cinar are with the Department of Aerospace Engineering, University of Michigan, Ann Arbor, MI, USA (e-mail: maxzli@umich.edu; cinar@umich.edu).

This work was supported by RTX under the Aircraft Design for Fleet Operations project.

A portion of this work was presented at 2025 IEEE Transportation Electrification Conference & Expo (ITEC) in Anaheim, CA on June 18, 2025 [1].

This is a preprint of the manuscript submitted to IEEE Transactions on Transportation Electrification. The manuscript has not yet been accepted for publication and may be subject to further revisions during the peer-review process.

discretizes each mission into 146 control points, enabling much higher-fidelity variation in power management across the entire flight envelope. This approach allows the mission profile itself—not only the power split—to adapt in pursuit of optimal energy usage. Furthermore, unlike many prior studies, the optimization framework developed here explicitly considers both fuel consumption and flight energy costs, capturing the influence of electricity pricing in addition to traditional fuel metrics.

Sequential power management and charging strategies have been studied in the context of UAVs [21]–[23], but the operational characteristics of regional HEA—including larger batteries, higher payloads, longer ranges, and stricter turnaround requirements—preclude direct transfer of UAV-based methods. A dedicated, high-fidelity study for regional aircraft is therefore required in the context of aircraft performance, propulsion system efficiency, and airline operations.

Previous work by the authors developed conventional and parallel-hybrid electric aircraft models based on the ERJ175LR regional jet using the Future Aircraft Sizing Tool (FAST) [13]. Analysis of regional airline route data from the Bureau of Transportation Statistics over a sequence of flights for a single tail number highlighted the impact of limited gate time on charging feasibility. Additionally, the findings revealed that hybridizing takeoff phase alone achieved approximately 2–3% fuel savings over conventional counterparts, while including climb hybridization imposed excessive battery weight, thereby resulting in higher fuel consumption than conventional aircraft. These outcomes were largely attributed to the use of a lower-fidelity engine model in the previous study. In this work, the engine model fidelity has been improved using the ICAO engine database method as detailed in [24].

The objective of this work is to develop an adaptive power management strategy for regional HEA that optimizes in-flight power distribution and ground charging across sequential daily missions. By dynamically allocating power between the electric motor and gas turbine engine over a finely discretized mission profile, while considering fuel burn and energy cost, the proposed strategy addresses real-world operational constraints while enhancing overall efficiency. This study fills a critical gap in current HEA literature by offering a scalable framework for trajectory-adaptive, cost-aware power management optimization, demonstrating its benefits for regional operations by reducing fuel consumption, while ensuring fleet compatibility.

II. Technical Approach

This section describes the technical methods used to develop the aircraft models, implement adaptive power management and dynamic battery charging strategies, and formulate both single-mission and sequence-based optimization problems.

A. Model Development and Design Mission Profile

Both conventional ERJ175LR and the HEA models were developed and analyzed using FAST[1], which is an open-source, MATLAB-based aircraft sizing tool for designing and analyzing conventional and electrified aircraft concepts across any propulsion architecture [24]. These models were sized on the design mission based on a notional ERJ175LR mission, as illustrated in Fig. 1. Each flight segment is defined by specified airspeeds and altitudes consistent with the ERJ175 mission profile (Table I). The mission profile includes a reserve mission to determine the required fuel capacity in compliance with FAA safety regulations [25]. For further details on the ERJ175LR model development, see [13].

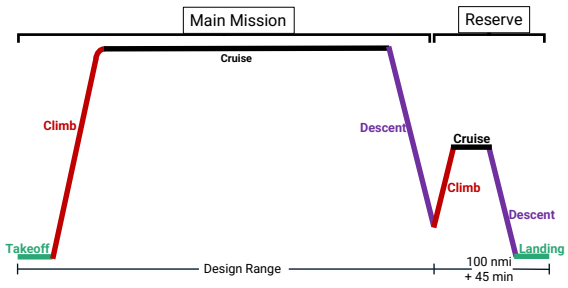

Fig. 1. Schematic of full mission profile in FAST.

TABLE I
Mission Profile Assumptions.

Segment Value	Main Mission	Reserve
Takeoff TAS (m/s)	69.5	-
Climb EAS (m/s)	102.9	102.9
Cruise TAS (m/s)	231.3	128.6
Cruise Altitude (m)	10668	3048
Descent EAS (m/s)	108.0	102.9
Landing TAS (m/s)	-	83.3

The HEA model integrates a parallel-hybrid propulsion architecture, illustrated in Fig. 2, into a twin-fan aircraft, with one battery back powering both electric motors. Hybridization is applied exclusively during takeoff and climb. The power outputs of the gas turbine engine (GT) and electric motor (EM) during climb are controlled via a throttle setting, or power code (PC), defined in (1). In off-design operations—where the aircraft design remains the same, but payload, range, and altitude targets differ from the design mission—the PC is used as an optimization variable to set the climb power output, allowing FAST to iteratively evaluate climb performance based on this control strategy. Takeoff always employs full throttle, ensuring maximum PC from all engines. Off-design missions follow the previously defined mission profile but adjust the design range and altitude to match the desired route, and all include the same reserve mission as shown in Fig. 1 and Table I.

$$P_{out} = PC \times P_{av}. \tag{1}$$

The following sections describe two optimization problems: one for single-mission power management and another for sequential-flight optimization that considers the effects of charging in between each flight. In both cases, FAST is treated as a black-box model, and finite difference methods are used for differentiation.

[1]https://github.com/ideas-um/FAST

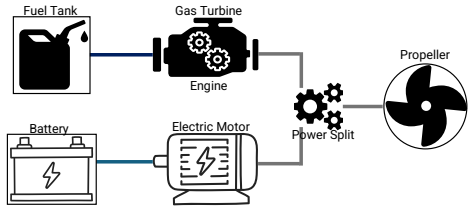

Fig. 2. Parallel-hybrid propulsion architecture.

B. Single Mission Optimization Problem

The single-mission optimizer minimizes the block fuel burn (W_f) by adjusting the power codes for the gas turbine engine $PC_{GT,i}$ and the electric motor $PC_{EM,i}$, where i denotes the i-th point in the discretized mission profile. During takeoff, both power sources operate at full throttle, while during climb the power codes vary continuously between 0% and 100%. Critical constraints include *(i)* maintaining the State of Charge (SOC) between 20% and 100% to ensure battery safety, *(ii)* limiting Rate of Climb (RC) to a prescribed maximum (RC_{max}) to maintain passenger comfort, *(iii)* ensuring that the required power to fly the given trajectory (P_{req}) does not exceed available power (P_{av}) from the propulsors, and *(iv)* keeping the takeoff gross weight ($TOGW$) within the maximum takeoff weight ($MTOW$) of the aircraft. The optimization problem statement is outlined below.

$$\begin{aligned} &\text{minimize} && W_f \\ &\text{by varying} && PC_{EM,i},\ PC_{GT,i}, \\ &\text{subject to} && 0\% \le PC_{EM,i} \le 100\%, \quad 0\% \le PC_{GT,i} \le 100\%, \\ & && 20\% \le SOC \le 100\%, \quad TOGW \le MTOW, \\ & && P_{\text{req},i} \le P_{\text{av},i}, \quad RC_i \le RC_{\max}. \end{aligned} \tag{2}$$

The optimization problem employs FAST with Matlab's *fmincon* function, utilizing nonlinear inequality constraints to solve for minimum fuel burn [26]. Interior-point method was chosen as the optimization algorithm due to its effectiveness in managing a large number of design variables, implementing non-linear constraints, converging even from an infeasible starting point, and locating the global minimum [27].

C. Sequence Optimization Problem

The sequence optimizer extends the single-mission approach to a full day of operations by optimizing the climb power codes for every mission in a flight sequence. An example sequence is illustrated in Fig. 3, which shows the design variable placements (PCs) across the discretized mission profiles and the time spent at the gate, partitioned into a fixed refueling period (first five minutes) and a subsequent charging period. The refueling time is estimated using a typical refueling truck fuel flow rate of 1000 kg/min for Jet A fuel [28].

The sequence-based optimization problem is summarized below. Its objective is to minimize the total daily fuel burn by accounting for energy usage in each flight and adjusting the SOC for subsequent missions through the charging phase. This

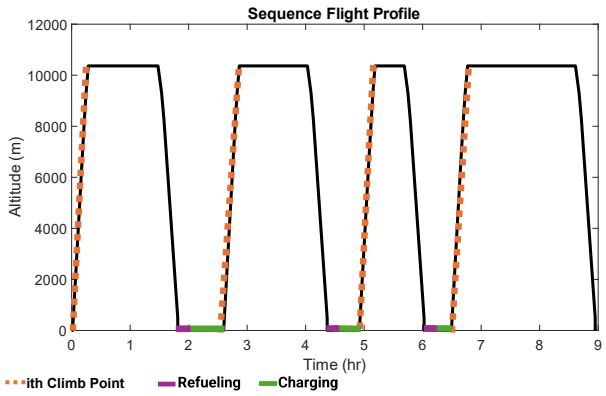

Fig. 3. Example sequence mission profile with discretized climb segment.

formulation allows the optimizer to balance energy depletion with battery state without imposing a fixed SOC threshold at the end of each mission. In this notation, k represents the mission number, ranging from 1 to n, where n is the total number of flights in the sequence.

Both optimization problems are set up to minimize fuel burn for the aircraft because it is hypothesized that fuel is the main contribution for operating cost. However, the value minimized can be changed to any aircraft model mission energy output like fuel energy, energy cost, or battery energy. The value minimized changes how the optimizer designates power code.

$$\begin{aligned} &\text{minimize} && \sum_{k=1}^{n} W_{f,k} \\ &\text{by varying} && PC_{\text{EM},k,i},\ PC_{\text{GT},k,i}, \\ &\text{subject to} && 0\% \le PC_{\text{EM},k,i} \le 100\%, \quad 0\% \le PC_{\text{GT},k,i} \le 100\%, \\ & && 20\% \le SOC_k \le 100\%, \quad TOGW_k \le MTOW, \\ & && P_{\text{req},k,i} \le P_{\text{av},k,i}, \quad RC_{k,i} \le RC_{\max}. \end{aligned} \tag{3}$$

D. Updates to FAST's Battery Model

This section summarizes the modifications implemented in FAST's battery model, which now incorporates maximum discharge rate checks during battery sizing and features a more realistic charging model. The specifications for the chosen Lithium-ion battery is given in Table II.

TABLE II
RECHARGEABLE LI-ION BATTERY PARAMETERS.

Parameter	Value	Unit
Cell Nominal Voltage (V_{nom})	3.6	V
Cell Maximum Capacity ($Q_{\max}$)	3	Ah
Battery Specific Energy (e_{batt})	250	Wh/kg
System Voltage (V_{system})	223.2	V
Maximum Allowable C-rate (C_{max})	5	C
Minimum SOC threshold	20	%
Cell Internal Resistance	0.0199	Ω
Cell Maximum Extracted Voltage	4.0880	V
Number of Cells in Series (N_{ser})	62	cells
Number of Cells in Parallel (N_{par})	372	cells

1) Battery Sizing Methodology: Battery sizing critically affects the aircraft gross weight, feasibility of the hybridization strategy, and the operational flexibility. In this study, the battery pack is sized iteratively within the aircraft sizing loop based on both the energy and power requirements of the design mission. First, the desired system voltage (V_{system}) and the nominal cell voltage (V_{Nom}), determine the number of cells in series (N_{ser}):

$$N_{ser} = \frac{V_{system}}{V_{Nom}}. \tag{4}$$

During aircraft sizing, the total required battery energy (E_{req}) and the maximum required battery power (P_{max}) are computed from mission analysis. For the power-based sizing, the maximum allowable discharge current ($I_{max,cell}$) is given by

$$I_{max,cell} = C_{max} \cdot Q_{max}, \tag{5}$$

which in turn is used to determine the number of parallel cells needed for power ($N_{par,power}$):

$$N_{par,power} = \frac{P_{max}}{V_{nom} \cdot N_{ser} \cdot I_{max,cell}}. \tag{6}$$

Similarly, the number of cells in parallel based on the energy requirement, $N_{par,energy}$, is

$$N_{par,energy} = \frac{E_{req}}{V_{nom} \cdot N_{ser} \cdot Q_{max}}. \tag{7}$$

The final battery pack design uses the most restrictive (largest) value, ensuring both energy and power criteria are met:

$$N_{par} = \max\left(N_{par,power}, N_{par,energy}\right). \tag{8}$$

An empirical equivalent circuit model captures the battery discharging dynamics by incorporating the open-circuit voltage (OCV) as a function of SOC, internal resistance, discharging current, polarization effects, and exponential voltage decay [13], [29]. The battery cell voltage during discharge is given by 9:

$$V_{disc} = V_0 - \left(\frac{K \cdot Q}{Q - Q_{act}}\right)(Q_{act} + I^*) - R \cdot I + Ae^{-B \cdot Q_{act}}, \tag{9}$$

where V_{disc} is the battery voltage, V_0 is the battery constant voltage, Q is the battery capacity, Q_{act} is the battery actual capacity, R is the internal resistance, I is the battery current, I^* is the filtered current, A is the exponential zone amplitude, B is the exponential zone time constant inverse, and K is the polarization constant.

2) Charging Strategy: A dynamic battery charging model was developed based on a constant current/constant voltage (CC-CV) strategy to capture the charging process with more fidelity given the time constraints. This enhancement replaces the simplified charging assumptions with industry standard protocols to improve the overall accuracy of energy management simulations and cost analysis. The battery is charged at the maximum allowable power, W_{max}, from the initial threshold until 80% SOC. Once the threshold is reached, it enters the CC phase at a constant current of 1C. Then, when the cutoff (maximum allowable) voltage is achieved, it switches to CV mode, where the voltage remains constant and the current gradually decreases until 0.02C [30], [31].

$$W_{ch} = \begin{cases} W_{max}, & 20\% \leq SOC < 80\%, \\ I_{const} V_{pack}(SOC), & 80\% \leq SOC < SOC_{CV}, \\ I_{dec}(t) V_{const}, & SOC_{CV} \leq SOC \leq 100\%, \end{cases} \tag{10}$$

V_{pack} is the actual loaded pack voltage at the corresponding SOC during CC phase, and I_{dec} is the tapering current during CV phase. Fig. 4 illustrates the charging profile.

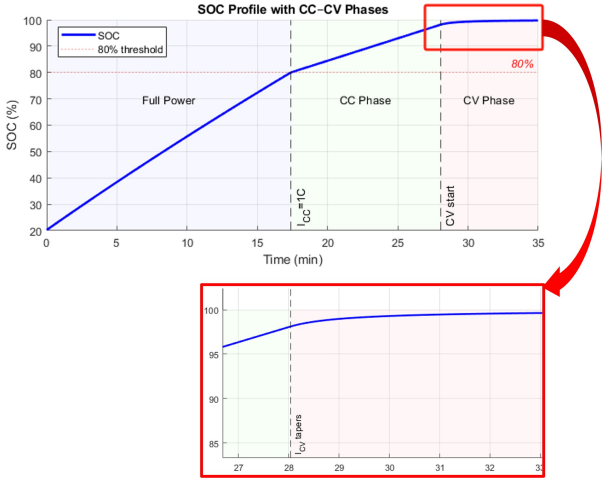

Fig. 4. Sample charging profile demonstrating constant power below 80% SOC, followed by the CC-CV strategy.

E. Flight Energy Cost

The optimization problems were expanded to consider flight energy cost as the objective function. The average cost of Jet A fuel and electricity for each state was collected from the US Energy Information Administration [32] [33]. The pricing data integrated into the sequence analysis to determine the cost of the flight based on refueling and recharging at the origin airport locations. An example of the pricing information by airport is provided in Table X.

TABLE III
EXAMPLE OF AIRPORT ENERGY PRICING.

Airport	City	Fuel Price ($/kWh)	Electricity Price ($/kWh)
ATL	Atlanta, GA	0.0692	0.1109
IAH	Houston, TX	0.0713	0.0881
MEM	Memphis, TN	0.0708	0.1213
PHL	Philadelphia, PA	0.0726	0.1101

Optimizing with respect to cost, rather than fuel burn, can provide additional insight on how differences between fuel and electricity pricing influence power management strategies. By incorporating cost into the optimization, this framework highlights cases where minimizing fuel burn and minimizing cost may not lead to identical power management strategies. Moreover, this cost-based formulation establishes a foundation for extending the framework to include future scenarios that capture influence of regional variation of electricity prices,

dynamic electricity prices, renewable energy penetration, or carbon pricing, providing a more complete perspective on the economic viability of regional HEA.

III. Results

This section summarizes the sizing outcomes of the aircraft models, verifies the convergence of the optimization framework, and applies the method to airline sequence case studies using 2019 Mesa Airlines operational data. Hybrid-electric aircraft performance is compared against a conventional ERJ175 baseline, focusing on fuel burn reduction and operating cost analysis to assess potential efficiency gains and economic impacts.

A. Model Design

Two aircraft models were developed based on the ERJ175LR top-level and mission performance requirements, as shown in Table IV. The HEA battery is modeled using current battery technology with a specific energy of 250 Wh/kg [34].

A prior study performed a sensitivity design analysis of the HEA to investigate different design power split strategies [35]. The study highlighted the trade-off between assigning a larger sea-level static (SLS) design power split to the electric motor and the resulting battery weight penalty. A higher electric share reduces the required gas turbine (GT) size, but as motor usage increases, the battery mass required offsets any fuel-burn benefits due to the added system weight.

For this work, the HEA configuration with the lowest overall fuel burn was selected. The propulsion system of the model is sized based on sea-level static (SLS) takeoff conditions, where 10% of the required power is provided by the electric motor, with the gas turbine supplying the remaining 90%, with both operating at maximum power code. During climb, the gas turbine continues at its maximum continuous power while the EM's power code is reduced to 30%. Sensitivity studies indicated that assigning a higher design SLS split at takeoff would result in an undersized GT for cruise performance, rendering it unable to complete the missing. A climb power code exceeding 30% necessitates an impractically heavy battery to support the entire climb segment leading to increased fuel burn. The resulting battery pack design, assuming a system voltage of 223V, is given in Table II.

B. Optimizer Verification

To verify the single-mission optimizer, a 1000 nmi off-design mission was used to assess whether fuel burn could be further reduced with adaptive power management while maintaining flight feasibility. A sensitivity study of varying input design variables confirmed that, within feasible bounds, the optimizer converged to the same optimal power management strategy (Table V). Compared to an HEA using the original design power codes, the optimized HEA reduced fuel burn by 1.7%.

Fig. 5 illustrates the climb power codes from the sized HEA model, which served as the initial design variables parameterized by climb altitude. The optimizer adjusted the gas turbine (GT) and electric motor (EM) power codes while ensuring the GT supports the mission climb and the EM operates between full throttle and off.

As shown in Fig. 6, the optimal solution follows an on–off–on EM strategy: the motor provides full support during takeoff, is deactivated at the start of climb, and is re-engaged at higher altitudes to expedite climb and transition to cruise. During the initial climb segment, the GT operates near maximum throttle, its most efficient condition, resulting in higher early fuel burn that reduces aircraft weight and conserves battery energy. At higher altitudes, GT thrust capability diminishes as the engine lapses; however, the conserved battery reserves allow the EM to deliver a full-power boost, maintaining climb rate and reaching cruise more efficiently.

TABLE IV
Conventional (Conv.) and HEA TLARs and Specifications.

Group	Specification	Conv.	HEA
ERJ175LR TLARs and Specifications	Design Range (nmi)	2150	2150
	Max Passengers	78	78
	Thrust-to-Weight Ratio	0.339	0.339
	Cruise Mach	0.78	0.78
	Wing Loading (kg/m^2)	533.4	533.4
	Cruise L/D	15.2	15.2
	Max RC (m/s)	11.43	11.43
Sized Aircraft Parameters	MTOW (kg)	38,637	41,147
	Empty Weight (kg)	21,545	23,093
	Block Fuel (kg)	9,397	9,364
	Battery Weight (kg)	–	996.4
	Total SLS Thrust (kN)	123.4	131.5
	SLS Engine Thrust (kN)	61.7	59.2
	Wing Area (m^2)	72.4	77.2
	Avg Takeoff Engine TSFC [kg/(kN·h)]	39.12	31.92
	Avg Cruise Engine TSFC [kg/(kN·h)]	70.62	65.08
	EM Power (kW)	–	913.0
	Battery Energy (kWh)	–	249.1

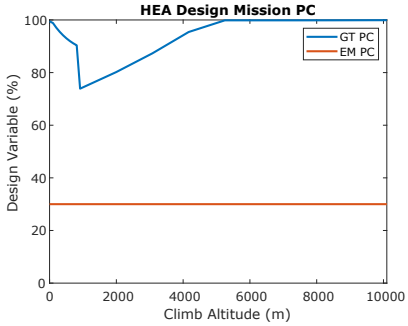

Fig. 5. Climb power codes from HEA model sized on design mission.

TABLE V
Initial Design Variable Convergence Sensitivity Study.

Initial Design Variables (%)		Min Fuel	Battery Energy
EM PC	GT PC	Burn (kg)	Used (kWh)
Design PC	Design PC	3,800.96	195
100	100	3,800.96	195
50	100	3,800.96	195
0	100	3,800.96	195

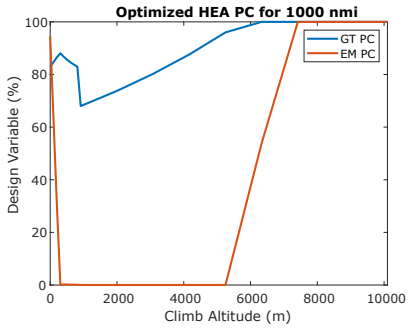

Fig. 6. Optimized climb power codes for a 1000 nmi mission.

C. Fuel Burn Comparison

The sequence in Table VI was selected from Mesa Airlines January 2019 flight data to capture diverse mission lengths and limited turnaround times [13]. Specifically, the first two flights are both long, testing whether the battery can be recharged sufficiently between them given minimal ground time. The schedule then includes two shorter flights followed by another long flight, further highlighting how varying mission lengths and charging intervals affect overall performance. The first flight begins at 100% SOC to represent overnight charging, and each airport is assumed to have a 150 kW charger, a realistic assumption considering current DC fast-charging technology [36].

TABLE VI
SELECTED REGIONAL AIRLINE SEQUENCE TO TEST AIRCRAFT OPERATIONAL PERFORMANCE.

Flight	**1**	**2**	**3**	**4**	**5**
Origin	IAH	PHL	IAH	MEM	IAH
Destination	PHL	IAH	MEM	IAH	TUS
Distance (nmi)	1,151	1,151	406.7	406.7	813.4
Cruise Altitude (m)	10365	10365	9,144	9,144	10365
Time at Gate (min)	0	37	65	53	50

Four test cases were examined to evaluate power management strategies, optimizer performance, and HEA benefits over its conventional counterpart:

- *Case 1.* HEA with power codes optimized across the entire sequence using Eqn 3.
- *Case 2.* HEA with power codes optimized for each individual missions and inter-flight charging using Eqn 2.
- *Case 3.* HEA using the original design power codes kept constant for all missions.
- *Case 4.* Conventional baseline model.

The total fuel burn and battery energy used for each case are reported in Table VII. Case 1 yields the lowest fuel burn and highest battery usage, while Case 3 saves only 1% fuel over the conventional baseline, highlighting the importance of employing optimized power management strategies.

Fig. 7 compares the design variables and SOC profiles across the sequence. In Cases 1 and 2, the EM operates at full throttle early in the climb and again near the top of climb to support the GT, which experienced reduced power available at higher altitudes. Table VIII summarizes the corresponding climb and flight times. In contrast, Case 3, which uses a constant 30% EM power, lacks sufficient top of climb boost, leading to a shallower, longer climb and higher total fuel burn. All HEA cases maintain a higher GT power code than the conventional baseline (Case 4), as the HEA's downsized gas turbine must operate at a higher throttle setting to provide the necessary thrust. Although the HEA carries additional battery weight, the enhanced cruise efficiency of the smaller engine more than compensates for this penalty, resulting in lower overall fuel consumption.

TABLE VII
FUEL AND BATTERY ENERGY CONSUMPTION OF CASES ON TEST SEQUENCE.

Case	**Total Fuel Burn (kg)**	**Fuel Burn Diff wrt Case 4**	**Total Battery Energy (kWh)**	**Total Energy Cost ($)**
1	14,674	-3.02%	635.5	12,677
2	14,697	-2.8%	635.3	12,697
3	14,974	-1.04%	556.6	12,798
4	15,131	-	-	12,906

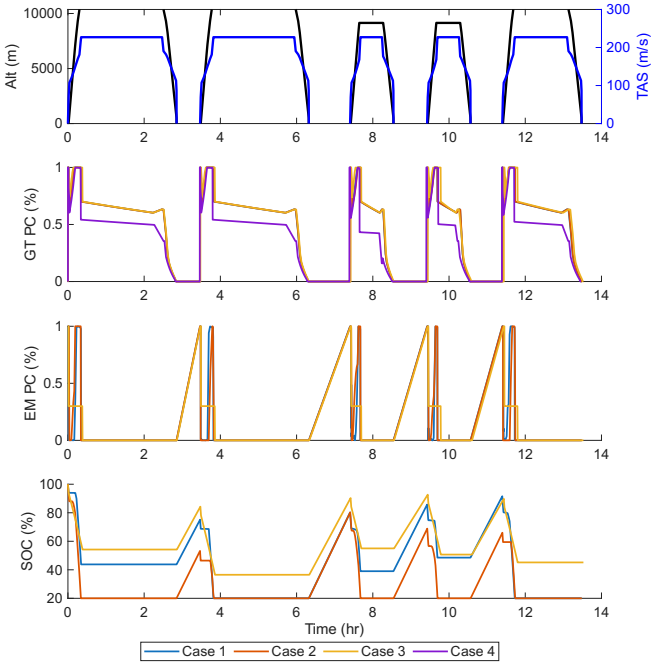

Fig. 7. Power codes and SOC for each case on the sequence.

TABLE VIII
TIME TO CLIMB AND FLY THE MISSION FOR EACH FLIGHT IN EACH CASE, PRESENTED IN MINUTES AS: CLIMB TIME; FLIGHT TIME.

	Case 1	**Case 2**	**Case 3**	**Case 4**
Flight 1	20.9; 171	20.4; 171	23.0; 172	20.3; 171
Flight 2	21.1; 171	22.5; 171	23.0; 172	20.3; 171
Flight 3	16.3; 68.3	16.2; 68.3	16.9; 68.5	16.1; 68.1
Flight 4	16.3; 68.3	16.2; 68.3	20.6; 69.8	16.1; 69.0
Flight 5	19.7; 125	20.3; 125	21.8; 125	19.6; 124

Between the two optimized approaches, Case 1 achieves greater fuel savings by prioritizing an 80% SOC before each flight. In contrast, Case 2 fully depletes the battery (to 20% SOC) on the first flight, leaving insufficient ground time to recharge beyond 55% SOC for the second flight. Consequently,

the EM cannot provide as much support during subsequent climbs, leading to a higher overall fuel burn than Case 1.

D. Future Technology Comparison

Under current battery technology, the HEA incurs a significant weight penalty, limiting its fuel-burn advantage. To explore the impact of improved batteries, a new HEA model was sized for the same TLARs and design mission, with a 500 Wh/kg battery. The resulting advanced HEA is summarized in Table IX.

TABLE IX
ADVANCED HEA SIZED WITH 500 WH/KG BATTERY ASSUMPTION.

Specifications	Value	% Change Over Conventional	% Change Over Current HEA
MTOW (kg)	38,244	-1.02	-7.06
Empty Weight (kg)	21,065	-2.23	-8.78
Block Fuel(kg)	9,027	-3.94	-3.60
Battery Weight (kg)	458.0	-	-54.03
Total SLS Thrust (kN)	122.2	-0.97	-7.09
SLS Engine Thrust (kN)	55.0	-10.86	-7.09
Wing Area (m^2)	71.7	-0.97	-7.12
EM Power (kW)	848.5	-	-7.06
Battery Energy (kWh)	229.0	-	-8.03

The resulting advanced HEA model was optimized over the same sequence (Case 5) with a high battery charging rate assumption of 500 kW. Case 5 reduced total fuel burn to 13,992 kg, which is -7.53% over Case 4 and -4.67% over Case 1, while using 892 kWh of battery energy. The power management of the optimized advanced and current technology HEA (Case 1) is compared in Fig. 8. Case 5 has an almost fully charged battery after every mission and uses higher electric motor power for longer during climb. This study shows that future technology levels will yield larger fuel burn reductions, and that power management optimization remains crucial to maximize the benefits because the mission profiles can vary widely. [37]

E. Energy Cost Comparison

The final optimization experiment performed is to minimize flight energy cost over the selected sequence. The energy costs for each sequence include the cost to refuel and recharge at the origin airport for each flight. This study provides insight on how electricity costs may impact optimal energy use. The current and advanced technology HEA power management strategy is again optimized on the sequence, Tab VI, to minimize total energy cost, Case 6 and 7 respectively. Their cost and energy use results are presented in Tab X and their power management strategies are compared to Case 1 and 5 in Fig 9.

TABLE X
OPTIMIZING POWER MANAGEMENT FOR LOWEST ENERGY COST SEQUENCE RESULTS.

Specifications	Case 6	Case 7
Total Fuel Burn (kg)	14,674	13,994
Total Energy Cost ($)	12,677	12,119
Total Battery Energy (kWh)	635.5	891.8

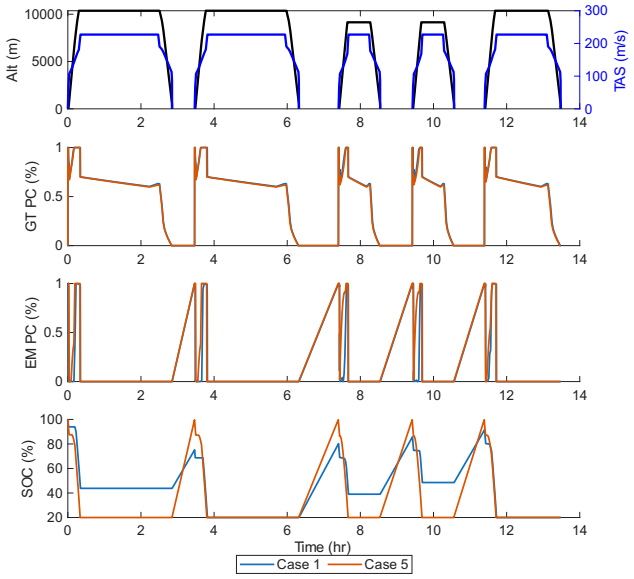

Fig. 8. HEA models with current and advanced technology optimized power management over sequence.

A deeper analysis of these results, particularly the nearly identical power management profiles in Figures 9 and 10, reveals a critical insight into the operational economics of current-generation HEA. Although electricity is often more expensive per kilowatt-hour than jet fuel at the airports studied, the optimizer still favors significant battery use during climb. This counterintuitive outcome arises because the primary driver of cost savings is not the marginal price of energy during climb, but the substantial fuel reduction achieved during the much longer cruise segment. By using electric assist during takeoff and climb, the HEA can be designed with a smaller gas turbine that operates closer to its peak efficiency point during cruise. The resulting fuel savings are so significant that they outweigh the higher cost of electricity, making the strategies for minimum fuel burn and minimum energy cost fundamentally the same under current U.S. market conditions.

IV. CONCLUSIONS

This study demonstrates that an adaptive power management strategy—one that dynamically allocates electric and gas turbine engine power across sequential flights—can achieve a 3% reduction in fuel burn and 2% in energy cost compared to conventional configurations. By integrating aircraft sizing with realistic operational constraints, including limited gate charging durations and variable mission profiles, the proposed approach enhances overall propulsive efficiency despite the additional battery weight imposed by current technology. Improved engine modeling using the ICAO engine database further strengthens these findings by enabling more accurate predictions of climb and cruise performance.

The results indicate that HEA can be feasibly integrated into regional airline fleets without disrupting existing operations, provided that power management is optimized to balance energy depletion and battery state effectively. Moreover, although the cruise phase does not operate in hybrid mode,

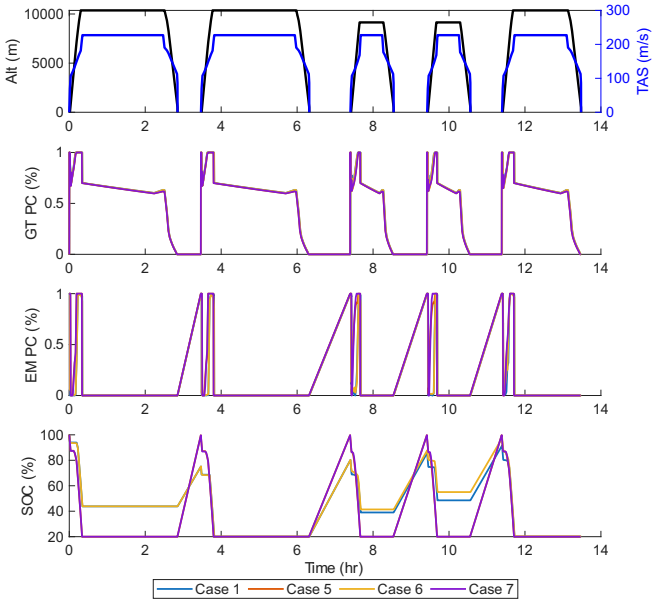

Fig. 9. HEA models optimized power management to minimize total energy cost compared to fuel burn.

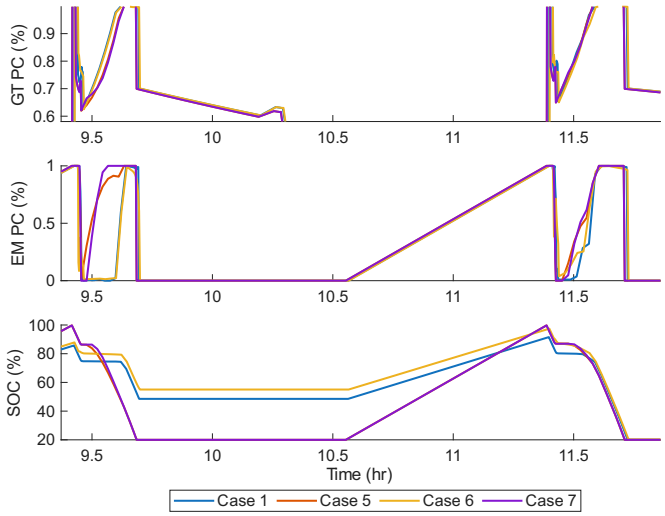

Fig. 10. Zoomed in power management strategy for last 2 missions.

the efficieny gains from operating a downsized gas turbine engine at a higher throttle setting compensate for the battery weight penalty. This leads to significant fuel savings during the dominant cruise segment.

Future work will expand battery model functions to include state of health monitoring and replacement costs estimations. The optimization problem can be expanded from flight energy cost to full life cycle cost of the aircraft in order to understand how power management effects the cost of the aircraft over its life.

ACKNOWLEDGMENTS

The authors thank Yi-Chih Wang and Paul Mokotoff for their contributions to this work; and Michael Ikeda for his role in the initial formulation of this research.

REFERENCES

[1] E. Cassidy, Y. Liu, M. Li, K. Kirsh, and G. Cinar, "Energy and power management optimization for sequential daily operations in regional hybrid-electric aircraft," in *ITEC+EATS 2025*, 2025.

[2] G. Cinar, Y. Cai, M. V. Bendarkar, A. I. Burrell, R. K. Denney, and D. N. Mavris, "System analysis and design space exploration of regional aircraft with electrified powertrains," *Journal of Aircraft*, vol. 60, no. 2, pp. 382–409, 2023. [Online]. Available: https://doi.org/10.2514/1.C036919

[3] M. Shi, G. Cinar, and D. N. Mavris, "Fleet analysis of a hybrid turboelectric commercial regional jet under nasa uli program," in *2021 AIAA/IEEE Electric Aircraft Technologies Symposium (EATS)*. IEEE, 2021, pp. 1–22.

[4] H. Abid, I. R. Skov, B. V. Mathiesen, and P. A. Østegaard, "Standalone and system-level perspectives on hydrogen-based sustainable aviation fuel pathways for denmark," *Energy*, vol. 320, p. 135450, 2025.

[5] A. Bills, S. Sripad, W. L. Fredericks, M. Singh, and V. Viswanathan, "Performance metrics required of next-generation batteries to electrify commercial aircraft," *ACS Energy Letters*, vol. 5, no. 2, pp. 663–668, 2020.

[6] C. L. Pastra, C. Dull, R. Berumen, C. Yumuk, G. Cinar, and D. N. Mavris, "Viability study of an electrified regional turboprop," in *2022 IEEE Transportation Electrification Conference & Expo (ITEC)*. IEEE, 2022, pp. 231–236.

[7] H. Kühnelt, F. Mastropierro, N. Zhang, S. Toghyani, and U. Krewer, "Are batteries fit for hybrid-electric regional aircraft?" *Journal of Physics: Conference Series*, vol. 2526, no. 1, p. 012026, jun 2023. [Online]. Available: https://dx.doi.org/10.1088/1742-6596/2526/1/012026

[8] C. Pornet and A. Isikveren, "Conceptual design of hybrid-electric transport aircraft," *Progress in Aerospace Sciences*, vol. 79, pp. 114–135, 2015. [Online]. Available: https://www.sciencedirect.com/science/article/pii/S0376042115300130

[9] B. Chan, Y. Deng, N. Tran, H. Wu, M. Ikeda, G. Cinar, and M. Li, "Optimizing fleet assignment decisions for regional airlines with hybrid electric aircraft uptake." International Council of Aeronautical Sciences 2024, aug 2024. [Online]. Available: https://www.icas.org/ICAS_ARCHIVE/ICAS2024/data/papers/ICAS2024_0781_paper.pdf

[10] J. Hoelzen, Y. Liu, B. Bensmann, C. Winnefeld, A. Elham, J. Friedrichs, and R. Hanke-Rauschenbach, "Conceptual design of operation strategies for hybrid electric aircraft," *Energies*, vol. 11, no. 1, 2018. [Online]. Available: https://www.mdpi.com/1996-1073/11/1/217

[11] International Air Transport Association (IATA), "Fact sheet: Fuel," 2019, accessed: 2025-08-26. [Online]. Available: https://www.iata.org/contentassets/25e5377cf53c4e48bbaa49d252f3ab03/fact-sheet-fuel.pdf

[12] C. Lents, Z. Baig, and R. Taylor, "Parallel hybrid propulsion secondary power system architecture exploration and evaluation," in *2020 AIAA/IEEE Electric Aircraft Technologies Symposium (EATS)*, 2020, pp. 1–7.

[13] Y. Deng, A. Kryuchkov, P. Mokotoff, E. Smith, J. Patel, S. Garcia Lavanchy, M. Z. Li, and G. Cinar, "Operational Analysis for Hybrid Electric Aircraft Fleets: A feasibility study for the short- and medium-haul markets," in *AIAA AVIATION 2023 Forum*. San Diego, CA and Online: American Institute of Aeronautics and Astronautics, jun 2023. [Online]. Available: https://arc.aiaa.org/doi/10.2514/6.2023-3868

[14] Y. XIE, A. SAVVARISAL, A. TSOURDOS, D. ZHANG, and J. GU, "Review of hybrid electric powered aircraft, its conceptual design and energy management methodologies," vol. 34, no. 4, pp. 432–450. [Online]. Available: https://www.sciencedirect.com/science/article/pii/S1000936120303368

[15] M. Rendón, C. Sánchez, J. Gallo Muñoz, and A. Anzai, "Aircraft hybrid-electric propulsion: Development trends, challenges and opportunities (https://rdcu.be/cmg4u)," *Sba Controle Automação Sociedade Brasileira de Automatica*, 06 2021.

[16] G. Cinar, Y. Cai, R. K. Denney, and D. N. Mavris, "Modeling and simulation of a parallel hybrid electric regional aircraft for the Electrified Powertrain Flight Demonstration (EPFD) program," in *IEEE/AIAA Transportation Electrification Conference and Electric Aircraft Technologies Symposium*, 2022.

[17] J. P. S. Pinto Leite and M. Voskuijl, "Optimal energy management for hybrid-electric aircraft," *Aircraft Engineering and Aerospace Technology*, vol. 92, no. 6, pp. 851–861, 2020.

[18] G. Palaia, K. Abu Salem, and E. Carrera, "Efficient methodology for power management optimization of hybrid-electric aircraft," *Aerospace*, vol. 12, no. 3, p. 230, 2025. [Online]. Available: https://www.mdpi.com/2226-4310/12/3/230

[19] K. I. Papadopoulos, C. P. Nasoulis, V. G. Gkoutzamanis, and A. I. Kalfas, "Flight-path optimization for a hybrid-electric aircraft," *Journal of Engineering for Gas Turbines and Power*, vol. 146, no. 7, p. 070902, 2024. [Online]. Available: https://asmedigitalcollection.asme.org/gasturbinespower/article/146/7/070902/1169251

[20] J. Zhang, I. Roumeliotis, and A. Zolotas, "Model-based fully coupled propulsion–aerodynamics optimization for hybrid electric aircraft energy management strategy," *Energy*, vol. 239, p. 123239, 2022. [Online]. Available: https://www.sciencedirect.com/science/article/pii/S0360544221019507

[21] P. Thantharate, A. Thantharate, and A. Kulkarni, "Greensky: A fair energy-aware optimization model for uavs in next-generation wireless networks," *Green Energy and Intelligent Transportation*, vol. 3, no. 1, p. 100130, 2024. [Online]. Available: https://www.sciencedirect.com/science/article/pii/S277315372300066X

[22] J. Hung and L. Gonzalez, "On parallel hybrid-electric propulsion system for unmanned aerial vehicles," *Progress in Aerospace Sciences*, vol. 51, pp. 1–17, 2012. [Online]. Available: https://www.sciencedirect.com/science/article/pii/S0376042112000097

[23] T. Kidd, Z. Yu, S. Dobbs, K. R. Anderson, G. Oetting, J. Kim, and M. O'Connell, "Uav power management, generation, and storage system principles and design," in *2020 IEEE Conference on Technologies for Sustainability (SusTech)*, 2020, pp. 1–8.

[24] P. Mokotoff, M. Arnson, Y.-C. Wang, and G. Cinar, "Fast: A future aircraft sizing tool for conventional and electrified aircraft design," in *AIAA SciTech 2025 Forum*, 2025, p. 2374.

[25] "14 cfr part 121 - operating requirements: Domestic, flag, and supplemental operations," *Code of Federal Regulations*, 2023, u.S. Federal Aviation Administration. [Online]. Available: https://www.ecfr.gov/current/title-14/chapter-I/subchapter-G/part-121

[26] *fmincon Documentation*. [Online]. Available: https://www.mathworks.com/help/optim/ug/fmincon.html

[27] J. Martins and A. Ning, *Engineering Design Optimization*, 10 2021.

[28] W. Industries, *Jet Refueler Spec Sheet*. [Online]. Available: https://superior.widen.net/s/lkgfqrjfrq

[29] O. Tremblay and L.-A. Dessaint, "Experimental validation of a battery dynamic model for ev applications," *World Electric Vehicle Journal*, vol. 3, no. 2, pp. 289–298, 2009. [Online]. Available: https://www.mdpi.com/2032-6653/3/2/289

[30] G. Ji, L. He, T. Wu, and G. Cui, "The design of fast charging strategy for lithium-ion batteries and intelligent application: A comprehensive review," *Applied Energy*, vol. 377, p. 124538, 2025.

[31] S. Duan, K. Xia, J. Li, Z. Zhao, and H. Liu, "Optimization charging method of lithium-ion battery based on multi-objective bbo algorithm," *Journal of Energy Storage*, vol. 91, p. 112046, 2024.

[32] U.S. Energy Information Administration, "Electric power monthly - average retail price of electricity," 2025, accessed: 2025-08-05. [Online]. Available: https://www.eia.gov/electricity/data/browser/#/topic/5?agg=2,0,1&geo=g&freq=M&start=200101&end=202505&ctype=linechart&ltype=pin&rtype=s&maptype=0&rse=0&pin=

[33] U. E. I. Administration, "State energy data system (seds): Petroleum prices, supply and demand information by state," https://www.eia.gov/state/seds/seds-data-fuel.php?sid=XX\#Petroleum, 2025, accessed: 2025-08-05.

[34] A. K. Koech, G. Mwandila, F. Mulolani, and P. Mwaanga, "Lithium-ion battery fundamentals and exploration of cathode materials: A review," *South African Journal of Chemical Engineering*, vol. 50, pp. 321–339, 2024. [Online]. Available: https://www.sciencedirect.com/science/article/pii/S1026918524001100

[35] E. Cassidy, P. R. Mokotoff, Y. Deng, M. Ikeda, K. Kirsch, M. Z. Li, and G. Cinar, "Design to deployment: Flight schedule-based analysis of hybrid-electric aircraft variants in u.s. regional carrier operations," 2025, mDPI Aerospace, accepted for publication.

[36] U.S. Department of Transportation, "Charging speeds," Sep 2023, accessed: 2023-10-21. [Online]. Available: https://www.transportation.gov/rural/ev/toolkit/ev-basics/charging-speeds

[37] A. Kamat, B. Chan, A. Sharma, H. Wu, E. Cassidy, K. Kirsch, G. Cinar, and M. Z. Li, "Full airline network fleet assignment model with hybrid electric aircraft uptake," *IEEE Transportation Electrification Conference & Expo (ITEC)*, IEEE, Anaheim, CA, June 2025.